

# Controlling harmonic generation in molecules with intense laser and static magnetic fields: Orientation effects

André D. Bandrauk and HuiZhong Lu

*Laboratoire de Chimie Théorique, Faculté des Sciences, Université de Sherbrooke, Sherbrooke, Québec, Canada J1K 2R1*

(Received 24 March 2003; published 20 October 2003)

We solve exactly the three-dimensional time-dependent Schrödinger equation for the  $H_2^+$  molecular ion in a combination of intense short laser pulses and static magnetic fields using a newly developed adaptive grid method. This allows for a study of the control of high-order harmonic generation in molecules by various orientations of the magnetic and laser fields in order to control electron recollision with nuclei. In particular, we find regimes of pure even harmonic or even and odd harmonic generation for particular field and frequency configurations. Furthermore, magnetic fields are found to extend harmonic generation plateaus to higher order as a result of further nonlinear coupling between charges and fields.

DOI: 10.1103/PhysRevA.68.043408

PACS number(s): 42.50.Hz

## I. INTRODUCTION

Atoms and molecules subjected to long-wavelength intense laser light emit high-order harmonics because of nonlinear, nonperturbative interaction of the electrons with the intense radiation field and the ion core. Plateaus with well-defined cutoffs are observed both experimentally [1] and in simulations [2–6] of high-order harmonic generation (HOHG). The physical mechanism for HOHG in atoms is now well understood. It has been shown that classical models apply and that electron rescattering of the ionized electron with the ion core is responsible for long plateaus and the cutoff [2,7,8]. Thus at high laser intensities, two physical parameters describe the energy acquired by an ionizing electron.

(i) The ponderomotive potential (1 a.u.=27.2 eV),

$$U_p \text{ (a.u.)} = eE^2/4m\omega^2 = 3.4 \times 10^{-21} I \text{ (W/cm}^2\text{)} \lambda^2 \text{ (nm)}. \quad (1)$$

(ii) The ponderomotive radius (1 a.u.=0.0529 nm),

$$\alpha \text{ (a.u.)} = eE/m\omega^2 = 2.4 \times 10^{-12} I^{1/2} \text{ (W/cm}^2\text{)} \lambda^2 \text{ (nm)}, \quad (2)$$

where  $E$  is the peak field strength of a laser of intensity  $I = cE^2/8\pi$  and frequency  $\omega$ .

The maximum number of harmonics  $N_m$  generated by an ionized electron in such a laser field has been shown theoretically [2–6] and experimentally [1] to obey the equation

$$N_m = (I_p + 3.17U_p)/\hbar\omega, \quad (3)$$

where  $I_p$  is the ionization potential and  $U_p$  [Eq. (1)], the ponderomotive energy, is the oscillating energy of the free electron in the electromagnetic field. As an example, at a wavelength  $\lambda = 1064$  nm (yttrium-aluminum-garnet laser) for which  $\omega = 0.0428$  a.u. (1.16 eV), then for the intensity  $I = 10^{14}$  W/cm<sup>2</sup>, one finds  $U_p = 10$  eV and  $\alpha_0 = 14$  Å. This readily gives  $N_m = 41$  photons. Clearly the field-induced oscillation energy  $U_p$  is comparable to the ionization energy  $I_p$  of an H atom (13.6 eV) or the molecular ion  $H_2^+$  (30 eV), two one-electron systems for which the time-dependent

Schrödinger equation (TDSE) can be solved exactly [9]. Thus the field-induced orbit  $\alpha$  [Eq. (2)] puts the electron well beyond the maximum influence of the Coulomb field. The effect of the laser field is to impose for linear polarization an oscillating amplitude  $\alpha \sin(\omega t)$  on the electron motion. This induces the electron to recollide with the nuclei at large wavelength. A classical [2] and semiclassical [7] theory reproduces well the maximum HOHG cutoff [Eq. (3)].

HOHG as predicted by Eq. (3) suggests that intense laser fields can be used to produce coherent ultraviolet (uv) and even x-ray radiation by going to even higher intensities and shorter pulses, resulting in attosecond pulses [10,11]. Thus stretching the plateau to higher energies is a highly desirable endeavor. One method to achieve higher cutoffs  $N_m$  has been suggested from numerical simulation: laser control of the ponderomotive radius  $\alpha$  [Eq. (1)] using a combination of two lasers,  $\omega + 3\omega$ , and varying the phase  $\phi$  between the two [4,5]. Thus using a combination of fields

$$E(t) = E_0[\cos(\omega t) + \delta \cos(3\omega t + \phi)], \quad (4)$$

we have been able to show that one can control in time the peak of the total laser field, and one can also control the returning trajectory  $\alpha$  of the electron in order to enhance HOHG. This has been generalized to create attosecond pulses [12,13].

Since the mechanism of HOHG in strong laser fields has been established to be a recollision of the electron with the ionic core induced by the laser field, limitations on the efficiency of HOHG have become evident. First, too high fields cause much ionization, i.e., the HOHG intensity saturates eventually [1]. However, one of the most serious problems is the expansion of the ionized electron wave packet as it oscillates back and forth in the laser's field [2]. In order to circumvent this problem and enhance the HOHG process, we have proposed earlier using a combination of intense laser and magnetic fields [14]. Basically, putting a magnetic field of strength  $B$  parallel to the electromagnetic field [15] puts the ionized electron in a magnetic “bottle,” thus squeezing the electron along the electric-field direction. In particular, numerical results for the  $H_2^+$  molecule from the exact TDSE for such a system have shown that one can indeed double the

HOHG spectrum to  $N_{\max}$  of about 100 with a magnetic field of about  $10^8$  G [14,15]. One intriguing aspect of this new approach is the fact that this doubling of the HOHG spectrum must arise from high-energy Landau levels, which are known to autoionize in an H atom as a result of nonseparability of the Coulomb plus magnetic-field system [16,17].

Current experiments at the Florida High Magnetic Field Research Facility hold the promise to achieve magnetic fields around  $10^6$  G with millisecond duration [18]. The crucial parameters in designing experiments to control electron recollision with nuclei using simultaneous intense electromagnetic and magnetic fields are the cyclotron radius  $R_B$  and frequency  $\omega_B$ , i.e.,

$$R_B = mv/e\gamma B_0, \quad \omega_B = \gamma B_0/m, \quad (5)$$

where  $\gamma = B/B_0$ ,  $B_0 = 2.35 \times 10^9$  G, the atomic unit of the magnetic field. Current available field strength corresponds to  $\gamma = 10^{-3}$ . We have previously proposed combinations of parallel intense short laser pulses and static magnetic fields in order to create a ‘‘magnetic bottle’’ along the internuclear  $R$  axis in order to increase HOHG [14] and charge resonance enhanced ionization (CREI) [16]. Such an approach has been generalized by adding also a static electric field in order to confirm the ‘‘three-step’’ model of HOHG in atoms [19]. Further progress in density-functional theory (DFT) has resulted in the generalization of the Kohn-Sham equations in order to include magnetic fields [20]. There is thus a growing theoretical framework to consider magnetic-field effects in molecules. In the present paper, we extend our previous work [14,15] in order to study a combination of short intense laser pulses of different polarization with static magnetic fields of different orientation. We present here solutions of the TDSE for 3D  $H_2^+$  (Born-Oppenheimer) using a newly developed adaptive grid method for time-dependent molecular problems [21]. Orientational and geometric effects on CREI in  $H_2^+$ ,  $H_2$ ,  $H_3^{2+}$ , and  $H_3$  have been previously examined numerically from the corresponding 2D TDSE [22,23,9] and this has been extended to HOHG [24]. We complete such previous studies by including magnetic-field effects.

## II. HOHG WITH CIRCULARLY POLARIZED LIGHT (x-y PLANE) AND MAGNETIC FIELD (z=R AXIS)

In our previous work on electron confinement by a magnetic field [14] in a 2D H atom, we examined the effect of a circularly polarized laser pulse perpendicular to a static magnetic field. Thus both laser and magnetic fields induce rotation about the same axis. Modulating the laser field frequency allowed for control of the high-order harmonic generation along one direction perpendicular to the magnetic field. In the present case, we generalize this example of laser control of HOHG for the  $H_2^+$  molecular ion.

We begin with the exact 3D Hamiltonian of  $H_2^+$  with static (Born-Oppenheimer) nuclei [3,5,6] adapted to the magnetic problem described above [16] (we use atomic units:  $e = \hbar = m_e = 1$ ),

$$i \frac{\partial \psi(x,y,z,t)}{\partial t} = [H_0 + H_I + H_B] \psi(x,y,z,t), \quad (6)$$

where

$$H_0 = -\frac{2m_p + 1}{4m_p} \left[ \frac{\partial^2}{\partial x^2} + \frac{\partial^2}{\partial y^2} + \frac{\partial^2}{\partial z^2} \right] - \frac{1}{[x^2 + y^2 + (z \pm R/2)^2]^{1/2}}, \quad (7)$$

$$\begin{aligned} H_I &= \kappa E_0 \cos(\omega t) [x \cos(\bar{\omega} t) + y \sin(\bar{\omega} t)] \\ &= \kappa \frac{E_0}{2} [x \cos((\omega + \bar{\omega})t) + y \sin((\omega + \bar{\omega})t)] \\ &\quad + \kappa \frac{E_0}{2} [x \cos((\omega - \bar{\omega})t) + y \sin((\omega - \bar{\omega})t)], \end{aligned} \quad (8)$$

$$\begin{aligned} H_B &= \beta \ell_z + \frac{1}{2} \beta^2 \rho^2 - \beta, \quad \ell_z = -i \left[ x \frac{\partial}{\partial y} - y \frac{\partial}{\partial x} \right], \\ \rho &= (x^2 + y^2)^{1/2}, \end{aligned} \quad (9)$$

and  $\kappa = (2m_p + 2)/(2m_p + 1)$ ,  $m_p = 1837$  is the mass of the proton,  $\beta = B/B_0$ , and  $B_0 = 2.35 \times 10^9$  G, the atomic unit of the magnetic field. We neglect here the effect of the magnetic field on the nuclear motion [25] since the resulting Lorentz force scales as  $v/c = \frac{1}{137}$  for one atomic unit (a.u.) of velocity and should therefore be negligible for the proton whose mass is 1837 a.u. Our model therefore consists of  $H_2^+$  aligned with the  $z$  axis in the presence of a static magnetic field of strength  $B$  parallel to  $z$  (internuclear axis  $R$ ). The magnetic field induces angular momentum  $\ell_z$  around the molecular axis and a confining potential  $\frac{1}{2} \beta^2 \rho^2$  perpendicular to that axis (the diamagnetic energy). The parameter that characterizes the magnetic confinement is the Landau radius due to harmonic motion in that confining potential, i.e.,  $R_L = (2/\beta)^{1/2}$ . Thus a magnetic field of strength  $\beta = 0.1$  ( $2.35 \times 10^8$  G) will induce a Landau radius  $R_L \approx 4.5$  a.u. around  $z$  ( $R$  – molecular axis). The modulated field in Eq. (8) corresponds to two circularly polarized fields which differ by  $2\bar{\omega}$  in frequency. At  $\omega = \bar{\omega}$ , this becomes a single circularly polarized field of frequency  $2\omega$  in the presence of a static electric field along the  $x$  axis.

Applying the unitary transformation  $T = \exp(-i\bar{\omega} t \ell_z)$ , which is a rotation around the  $+z$  direction by the angle  $\bar{\omega} t$ , gives the new Hamiltonian

$$H' = H_0 + \frac{1}{2} \beta^2 \rho^2 + (\beta - \bar{\omega}) \ell_z + x E_0 \cos(\omega t). \quad (10)$$

The new Hamiltonian exhibits a magnetic confinement potential  $\frac{1}{2} \beta^2 \rho^2$ , a rotation term  $(\beta - \bar{\omega}) \ell_z$ , and a linear driving field term  $x E_0 \cos(\omega t)$  in the frame rotating at frequency  $\bar{\omega}$ . This last term will give rise to a ponderomotive energy  $U_p$ , Eq. (1). The model of HOHG via recollision of the ionized electron with the ion core predicts a maximum harmonic order given by Eq. (3) [2,6–8]. We note here that since  $x$  is not diagonal in the angular momentum quantum

number  $m$  (around the  $z$  axis), the last laser-driving term in Eq. (10) couples different angular momentum terms, thus also pumping energy into circular motion.

In the present paper, we use another approach in order to simplify the numerical procedure to solve the TDSE (6). We eliminate the Larmor (magnetic) rotation  $\beta\ell_z$  by the coordinate transformation,

$$\begin{aligned}\bar{x} &= +x \cos(\beta t) + y \sin(\beta t), \\ \bar{y} &= -x \sin(\beta t) + y \cos(\beta t),\end{aligned}\quad (11)$$

$$\bar{z} = z.$$

This transformation implies the rotation

$$\frac{\partial \bar{x}}{\partial t} = \beta \bar{y}, \quad \frac{\partial \bar{y}}{\partial t} = -\beta \bar{x}, \quad (12)$$

i.e., rotation around  $z$  at the frequency  $\beta$  instead of  $\bar{\omega}$  as in Eq. (10). Using the new coordinate system, the TDSE (6) becomes

$$i \frac{\partial \psi(\bar{x}, \bar{y}, z, t)}{\partial t} = [H_0 + \frac{1}{2} \beta^2 \rho^2 - \beta] \psi(\bar{x}, \bar{y}, z, t) + \kappa E_0 \cos(\omega t) [\bar{x} \cos((\bar{\omega} - \beta)t) + \bar{y} \sin((\bar{\omega} - \beta)t)] \psi(\bar{x}, \bar{y}, z, t). \quad (13)$$

We note that  $H_0$  in Eq. (6) remains unchanged. An advantage of the new TDSE (13) as compared to Eq. (10) is that the linear laser driving term is no longer confined to one direction, the  $x$  axis, but involves now time-dependent variables  $\bar{x}, \bar{y}$ , Eq. (11), which depend on the magnetic-field strength  $\beta$  and are circular in the  $x$  and  $y$  coordinates. We note that at  $\beta = \bar{\omega}$ , both Eqs. (10) and (13) become equivalent with  $x$  transformed to  $\bar{x}$ .

The new TDSE, Eq. (13), is solved using our new adaptive grid numerical method developed to treat molecular 3D problems in Cartesian coordinates [21]. Calculation of the HOHG spectrum is achieved by calculating the time-dependent average value of the induced dipoles [3,26] from the exact wave function  $\psi(x, y, z, t)$ ,  $d(t) = \langle \psi | d | \psi \rangle$ , with components

$$\begin{aligned}x(t) &= \bar{x} \cos(\beta t) - \bar{y} \sin(\beta t), \\ y(t) &= \bar{x} \sin(\beta t) + \bar{y} \cos(\beta t).\end{aligned}\quad (14)$$

Fourier transforming these time-dependent dipoles to frequency allows us to reconstruct the power spectrum  $|d(\omega)|^2$ .

We have performed calculations at the intensity  $I_0 = 10^{15}$  W/cm<sup>2</sup> corresponding to an electric-field strength  $E_0 = 0.16885$  a.u., wavelength  $\lambda = 800$  nm or frequency  $\omega = 0.057$  a.u., and magnetic-field strength  $\beta = 0.1$  a.u. giving rise to a Landau confinement radius  $R_L = (2/\beta)^{1/2} = 4.5$  a.u. The corresponding ponderomotive energy is  $U_p = E_0^2/4\omega^2 = 2.2$  a.u. =  $39\omega$ . We present results at the equilibrium distance of  $\text{H}_2^+$ ,  $R = 2$  a.u. so that the ionization potential  $I_p \approx 0.5 + 1/R \approx 1$  a.u. =  $17.6\omega$ . Therefore, for linearly polarized light, the maximum number of harmonics expected is from Eq. (3),  $N_m \approx 140$ . Calculations have been performed with a linear pulse rise of five cycles (one cycle = 2.7 fs) and then a constant field to 25 cycles.

We illustrate in Fig. 1 the HOHG spectrum along the  $x$  direction perpendicular (the  $y$  direction is identical) to the  $z$  (internuclear) axis for magnetic-field strength  $\beta = 0.1$  and  $\bar{\omega} = \beta > \omega$  (i.e.,  $\bar{\omega} = 0.1$  a.u. =  $1.75\omega \approx 450$  nm) at  $I = 10^{15}$  W/cm<sup>2</sup>,  $\lambda = 800$  nm. The inset shows the fine struc-

ture appearing at low harmonic order. We note that  $\bar{\omega} + \omega = 2.75\omega$ ,  $\bar{\omega} - \omega = 0.75\omega$ . The splitting observed corresponds to the frequency difference  $\Delta \approx 2(\bar{\omega} - \omega)$ , since two frequencies  $\bar{\omega} + \omega$  and  $\bar{\omega} - \omega$  are exciting the molecule. The spectrum shows minima and maxima arising from interferences between different recolliding electron trajectories, which are expected to occur in the low  $\omega$  frequency range used here [2,6,19]. However, no sharp cutoff or maxima  $N_m$  are observed in the circularly polarized case with a magnetic field. Thus a maximum around  $N_m = I_p + 2U_p = 95\omega$ , expected for ionized but confined (by the diamagnetic energy) electrons, is found to be followed by further progression of the harmonic spectrum. This is an indication of the original idea that a combination of magnetic fields and laser fields should enhance energy pumping into ionized electrons and extend HOHG plateaus for both linearly polarized and circularly polarized laser fields [14]. This is achieved by confinement of the ionized electron by the magnetic field and the motion is mainly in the  $x$  direction, Eq. (10).

The above nondegenerate frequency configuration, where  $\omega + \bar{\omega} = 2.75\omega$ ,  $\bar{\omega} - \omega = 0.75\omega$ , and  $\bar{\omega} = \beta = 1.75\omega$ , produces

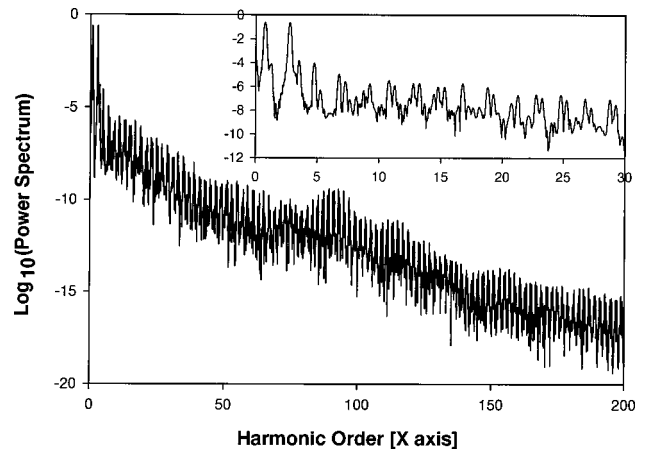


FIG. 1.  $x$ -axis HOHG spectrum for  $I = 10^{15}$  W/cm<sup>2</sup>, in the  $x$ - $y$  plane:  $\bar{\omega} = \beta = 0.1$  a.u.;  $\omega = 0.057$  a.u. ( $\lambda = 800$  nm) for 3D  $\text{H}_2^+$  at  $R = 2$  a.u.

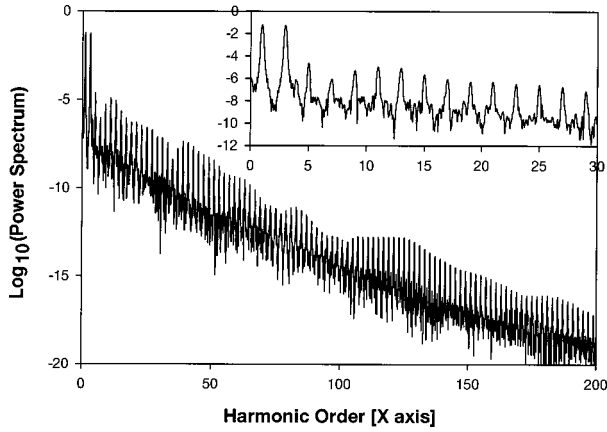


FIG. 2.  $x$ -axis HOHG spectrum for  $I = 10^{15}$  W/cm<sup>2</sup>, in the  $x$ - $y$  plane:  $\bar{\omega} = \beta = 0.114$  a.u. =  $2\omega$ ;  $\omega = 0.057$  a.u. ( $\lambda = 800$  nm).

only *odd* harmonics that are split due to the sum and difference frequencies  $\bar{\omega} + \omega$  and  $\bar{\omega} - \omega$ . Changing now to the degenerate regime  $\bar{\omega} = \beta = 2\omega$  produces effective field frequencies  $\bar{\omega} + \omega = 3\omega$  and  $\bar{\omega} - \omega = \omega$ . In our previous study of HOHG control without magnetic fields, such  $\omega + 3\omega$  combination with linear polarization was shown to lead to a small extension of plateaus beyond the classical  $N_m$  law (3) [4,5]. In Fig. 1 corresponding to the nondegenerate case, high intensities and much longer harmonic progressions are obtained with no definite cutoff. In the present degenerate case, long progression persists but intensities are much lower, Fig. 2. We surmise that this is due to the fact that the Larmor frequency,  $\beta = 2\omega$ , is now nonresonant with the effective laser frequencies  $3\omega$  and  $\omega$ . We note further that due to the commensurate frequencies  $\omega, 2\omega, 3\omega$  present no splitting of the odd-only harmonics occurs, Fig. 2.

We confirm this hypothesis by presenting in Fig. 3 the completely degenerate case  $\omega = \bar{\omega} = \beta/2 = 0.057$  a.u. One effective laser frequency,  $\bar{\omega} + \omega = \beta$ , appears now since  $\omega - \bar{\omega} = 0$ . Thus from Eq. (8) we note that this degenerate frequency configuration corresponds to a single circularly polarized field at frequency  $\beta$  in the  $x$ - $y$  plane in resonance with the Larmor frequency  $\beta$  and in the presence of a static elec-

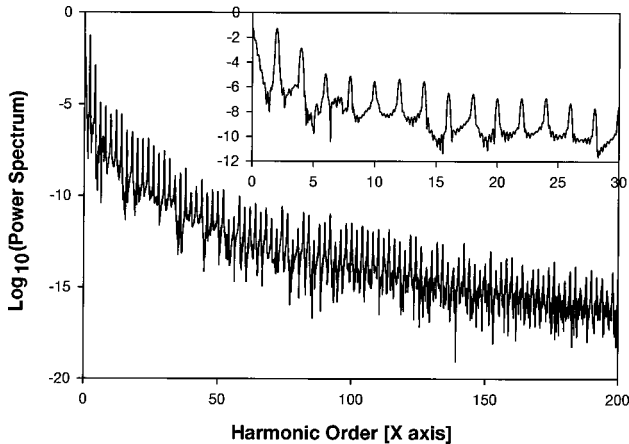


FIG. 3.  $x$ -axis HOHG spectrum for  $I = 10^{15}$  W/cm<sup>2</sup>, in the  $x$ - $y$  plane:  $\bar{\omega} = \omega = 0.057$  a.u.;  $\beta = 2\omega = 0.114$  a.u.

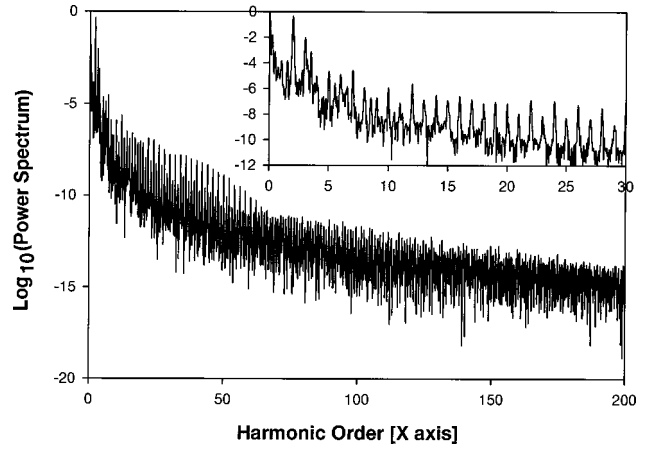


FIG. 4.  $x$ -axis HOHG spectrum for  $I = 10^{15}$  W/cm<sup>2</sup>, in the  $x$ - $y$  plane:  $\bar{\omega} = \omega = 0.057$  a.u.;  $\beta = 0.1$  a.u.

tric field along the  $x$  axis. The net effect is to produce a pure *even* HOHG spectrum and no line splittings, Fig. 3. Since in a zero magnetic field, HOHG with a single circularly polarized laser field is not possible due to photon momentum conservation, the present configuration, where the frequency of the circularly polarized laser is resonant with the magnetic Larmor frequency  $\beta$ , introduces copious harmonics (no visible cutoff in Fig. 3) which are all even. The magnetic field thus creates Zeeman levels whose energy separation is precisely  $\beta$  [Eq. (9)], which are excited by single-photon transition at frequency  $\omega + \bar{\omega} = 2\omega = \beta$ . This appears as *even* harmonics; however, we emphasise that it is the presence of the magnetic field and the static electric field which creates the even HOHG spectrum. Comparing Figs. 1, 2, and 3, in the first two Figures only *odd* harmonics appear since no sum  $\omega + \bar{\omega}$  or difference  $\bar{\omega} - \omega$  frequency [Eq. (8)] is resonant with the Larmor frequency  $\beta$ , whereas in Fig. 3 only *even* harmonics appear since the sum frequency  $\omega + \bar{\omega}$  is equal to  $\beta$ . The sensitivity to resonant and nonresonant conditions is further confirmed in Fig. 4, where we show the HOHG spectra for  $\omega = \bar{\omega} = 0.057$  and  $\beta = 0.1$ . Since  $\omega + \bar{\omega} = 0.114$  whereas  $\bar{\omega} - \omega = 0$ , we find now that both even and odd harmonics appear simultaneously with near equal intensity in this nondegenerate case because of the presence of a static electric field along the  $x$  axis [Eq. (8)]. The HOHG spectrum shows again a very extended spectrum with no visible cutoff corresponding to Eq. (3).

### III. HOHG WITH CIRCULARLY POLARIZED LIGHT (y-z PLANE) AND MAGNETIC FIELD (x AXIS)

We now generalize the previous perpendicular laser polarization and magnetic-field orientation to  $y$ - $z$  plane confinement, where  $z \parallel R$  is the molecular internuclear axis. For the laser-molecule interaction  $H_I$  we now write

$$H_I = \kappa E_0 \cos(\omega t) [y \cos(\bar{\omega} t) + z \sin(\bar{\omega} t)] \quad (15)$$

with  $\bar{\omega} = \beta$ , the Larmor frequency. This Hamiltonian represents laser-induced rotation of the electron in the  $y$ - $z$  plane, so that the electron can now in principle *collide* with the

protons separated by distance  $R$  along the  $z$  axis. This is a generalization of the laser-induced recollision model [2] applied now to molecules [6]. The magnetic field is chosen to be oriented along the  $x$  axis in order to enhance or hinder the laser-induced electron rotation in the  $y$ - $z$  plane, where  $\ell_x = -i[y(\partial/\partial z) - z(\partial/\partial y)]$ . Applying the unitary transformation  $T = \exp(-i\bar{\omega}t\ell_x)$  gives the new Hamiltonian from Eqs. (6) and (15),

$$H = H_0 + \frac{1}{2}\beta^2(y^2 + z^2) + (\beta - \bar{\omega})\ell_x + yE_0 \cos(\omega t). \quad (16)$$

From Eq. (16) we see now the appearance of the diamagnetic confinement term and rotation in the  $y$ - $z$  plane. In this rotating frame, the electron is now being driven along the  $y$  axis.

---


$$H_0 = -\frac{2m_p + 1}{4m_p} \left( \frac{\partial^2}{\partial \bar{x}^2} + \frac{\partial^2}{\partial \bar{y}^2} + \frac{\partial^2}{\partial \bar{z}^2} \right) - \{ \bar{x}^2 + \bar{y}^2 + (\bar{z} \pm R/2)^2 \} \pm R[\bar{y} \sin(\beta t) + \bar{z} \cos(\beta t)]^{-1/2}, \quad (19)$$

and the new TDSE in the new coordinates  $(\bar{x}, \bar{y}, \bar{z})$ ,

$$i \frac{\partial \psi(\bar{x}, \bar{y}, \bar{z}, t)}{\partial t} = \{ H_0 + \frac{1}{2}\beta^2(\bar{y}^2 + \bar{z}^2) - \beta + \kappa E_0 \cos(\omega t)[\bar{y} \cos((\bar{\omega} - \beta)t) + \bar{z} \sin((\bar{\omega} - \beta)t)] \} \psi(\bar{x}, \bar{y}, \bar{z}, t). \quad (20)$$

In this new rotating coordinate system, the protons rotate themselves at positions  $(\bar{y}, \bar{z}) = \pm(R/2)(\sin \beta t, \cos \beta t)$ . Solving the TDSE (20) allows us to calculate the time-dependent averages, e.g.,  $\langle \psi(\bar{x}, \bar{y}, \bar{z}, t) | d | \psi(\bar{x}, \bar{y}, \bar{z}, t) \rangle$ , of the induced dipoles,

$$\begin{aligned} y(t) &= \bar{y}(t) \cos(\beta t) - \bar{z}(t) \sin(\beta t), \\ z(t) &= \bar{y}(t) \sin(\beta t) + \bar{z}(t) \cos(\beta t). \end{aligned} \quad (21)$$

Fourier transforming these laser-induced dipoles gives the power spectrum  $|d(\omega)|^2$  as a function of the frequency  $\omega$ .

We examine first the case  $\bar{\omega} = \beta = 0.1$ ,  $\omega = 0.057$  for which from Eqs. (16) and (20) the main effect of the electromagnetic field is to drive the electron along the  $y$  direction in the  $y$ - $z$  rotating frame. Figure 5 shows the corresponding HOHG spectrum in the  $z$  direction ( $y$ - $z$  plane). This is to be compared to Fig. 1 where the effective driving motion of the electron is in the  $x$  direction but in the  $(x$ - $y)$  plane, Eq. (10). In the latter case, only odd harmonics split into two— $\bar{\omega} + \omega = 2.75\omega$ ,  $\bar{\omega} - \omega = 0.75\omega$ —appear, whereas in Fig. 5 both even and odd split harmonics now appear simultaneously with equal intensity. Thus Fig. 5 corresponds to all even and odd harmonics split in two, whereas Fig. 1 contains only the odd harmonics with the same splittings,  $\bar{\omega} + \omega$  and  $\bar{\omega} - \omega$ . The HOHG spectrum in the  $y$  direction is identical to the  $z$  spectrum. We note that the even-odd harmonic spectrum in Fig. 5 as compared to the odd harmonic spectrum only in Fig. 1 reflects some symmetry breaking in the first, i.e., in the configuration where both counter-rotating circularly polarized laser fields and the magnetic field are perpendicular

As in the previous  $x$ - $y$  plane regime, we choose rotating coordinates in order to eliminate angular momentum terms in the Hamiltonian (16). Thus setting

$$\begin{aligned} \bar{x} &= x, \\ \bar{y} &= y \cos(\beta t) + z \sin(\beta t), \\ \bar{z} &= -z \sin(\beta t) + z \cos(\beta t), \end{aligned} \quad (17)$$

which implies

$$\frac{\partial \bar{y}}{\partial t} = \beta \bar{z}, \quad \frac{\partial \bar{z}}{\partial t} = -\beta \bar{y}, \quad (18)$$

we obtain the transformed Hamiltonian  $H_0$ ,

---

to each other ( $y$ - $z$  plane and  $x$  axis) but the electron now circulates in the molecular plane ( $y$ - $z$  plane). This symmetry breaking can be seen clearly by comparing the rotation frame equations (13) and (19). Thus in Fig. 1, at frequency  $\bar{\omega} = \beta$ , the electron is driven along the  $\bar{x}$  axis but the field-free Hamiltonian  $H_0$  is symmetry-conserving in the  $x$ - $y$  rotating frame. In the second case, Fig. 5, the field-free Hamiltonian  $H_0$  (19) is non-symmetry-conserving in the rotating  $y$ - $z$  plane, with the nuclei now rotating themselves with coordinates  $(\bar{y}, \bar{z})$ .

We next compare the case  $\bar{\omega} = \beta = 2\omega$ , where  $\omega = 0.057$ . Thus for the ( $y$ - $z$ ) plane laser polarization— $x$ -axis magnetic-field direction this is shown in Fig. 6 for HOHG along the  $z$

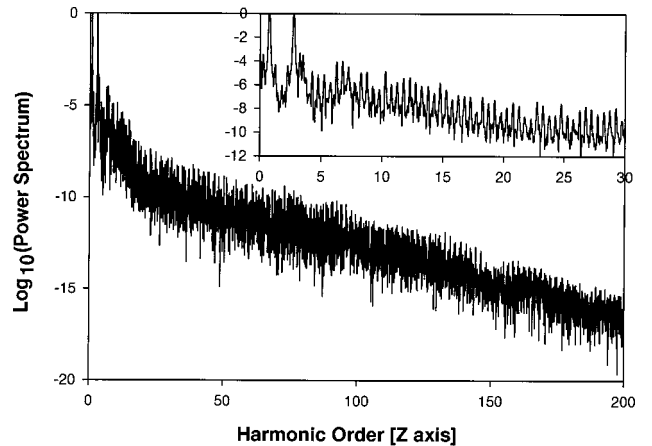


FIG. 5.  $z$ -axis HOHG spectrum for  $I = 10^{15}$  W/cm<sup>2</sup>, in the  $y$ - $z$  plane:  $\bar{\omega} = \beta = 0.1$  a.u.;  $\omega = 0.057$  a.u. ( $\lambda = 800$  nm).

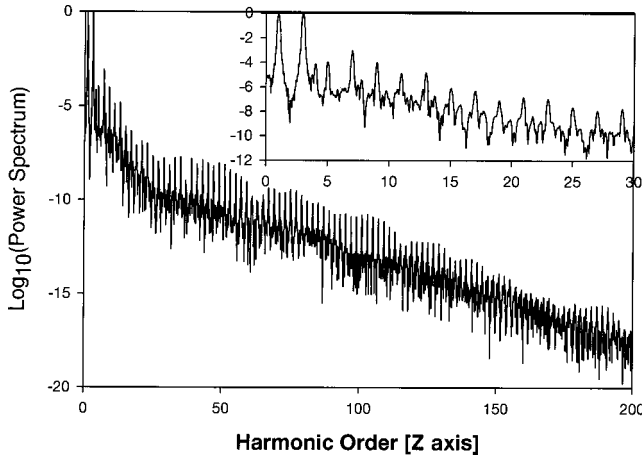


FIG. 6.  $z$ -axis HOHG spectrum for  $I=10^{15}$  W/cm<sup>2</sup>, in the  $y$ - $z$  plane:  $\bar{\omega}=\beta=0.114$  a.u. =  $2\omega$ ,  $\omega=0.057$  a.u.

axis (the  $y$  axis gives similar results). When compared to the identical laser–magnetic-field parameters but ( $x$ - $y$ ) plane and  $z$  axis configurations, Fig. 2, one basically obtains the same spectrum especially in the details (see the insets of Figs. 2 and 6). Only odd harmonics appear with similar intensities, i.e., intense first and third harmonics, followed by a long plateau. Thus although from Eq. (16) one would expect that at  $\bar{\omega}=\beta$  the magnetic coupling vanishes in the rotating frame for both Figs. 5 and 6, thus producing similar HOHG spectra, we must emphasize that in Fig. 5,  $\bar{\omega}=\beta\neq\omega$ , whereas in Fig. 6,  $\bar{\omega}=\beta=2\omega$ . Thus in both cases, the magnetic coupling term  $(\beta-\bar{\omega})l_x$ , Eq. (16), vanishes, but the commensurability  $\bar{\omega}=2\omega$  results in two effective laser fields with frequencies  $\omega+\bar{\omega}=3\omega$  and/or  $\bar{\omega}-\omega=\omega$  in the  $\bar{y}$  direction, Eq. (20) for Fig. 6, and in the  $\bar{x}$  direction, Eq. (13) and Fig. 2. Thus both figures are similar due to the similar physical effects in the rotating frames [Eq. (20) versus Eq. (13)].

We next examine the case  $\omega=\bar{\omega}=0.057$ ,  $\beta=2\omega$ , Fig. 7, for the  $y$ - $z$  plane laser polarization,  $x$ -axis magnetic-field direction compared to Fig. 3 for the same parameter but  $x$ - $y$  polarization,  $z$ -axis magnetic direction. Both spectra are quite similar with only *even* harmonics appearing. Finally, we il-

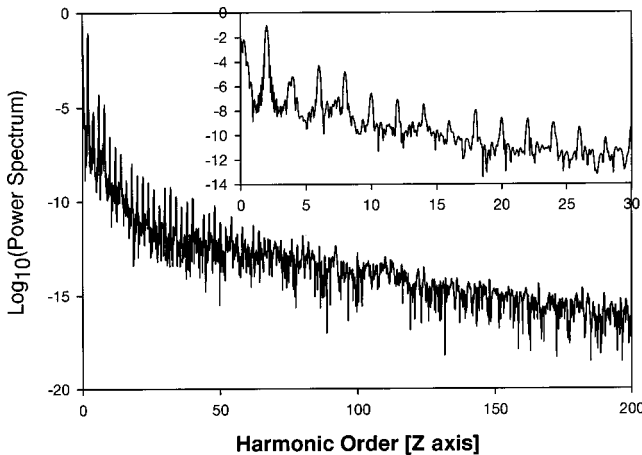


FIG. 7.  $z$ -axis HOHG spectrum for  $I=10^{15}$  W/cm<sup>2</sup>, in the  $y$ - $z$  plane:  $\bar{\omega}=\omega=0.057$  a.u.;  $\beta=2\omega=0.114$  a.u.

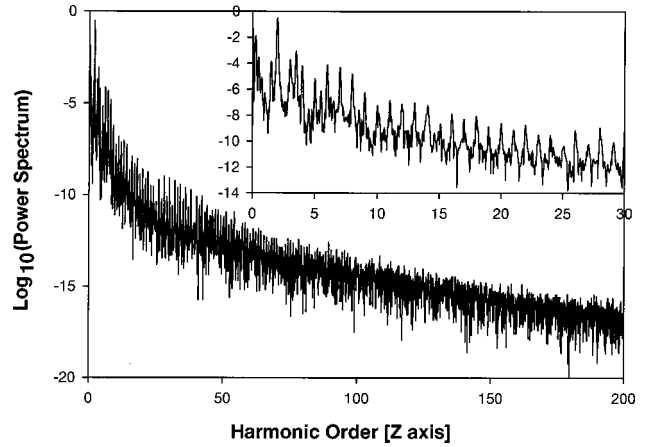


FIG. 8.  $z$ -axis HOHG spectrum for  $I=10^{15}$  W/cm<sup>2</sup>, in the  $y$ - $z$  plane:  $\bar{\omega}=\omega=0.057$  a.u.;  $\beta=0.1$  a.u.

lustrate in Fig. 8 the case  $\bar{\omega}=\omega=0.057$ ,  $\beta=0.1$ , the complete incommensurate case and  $y$ - $z$ ,  $x$  configuration versus Fig. 4 for the same laser parameters but the  $x$ - $y$ ,  $z$  configuration. The HOHG spectrum is nearly identical in both cases with both even and odd harmonics appearing simultaneously.

#### IV. CONCLUSION

One of the fundamental concepts in understanding HOHG generation efficiencies is the recollision model of the ionized electron with its parent ion [2] or with neighboring ions in extended systems such as molecules or clusters [3]. Low efficiencies of HOHG are due to the electron wave packet spreading upon recollision [1,2] after tunneling. Magnetic fields can thus be used to squeeze, i.e., inhibit such wave-packet spreading, with the result that the HOHG efficiency can be somewhat increased [5,14,19]. Furthermore, the magnetic bottle effect has helped confirm the recollision model of HOHG [5,19]. In the present paper, we have examined the effect of various orientations or configurations of intense short circularly polarized laser pulses and magnetic fields. In particular, we have examined a combination of two circularly polarized pulses which differ in frequency by  $2\bar{\omega}$ , where  $\bar{\omega}$  can be tuned to the Larmor frequency  $\beta$  of magnetic rotation induced by a magnetic field  $B$  perpendicular to the plane of circular polarization. It is in this configuration that the magnetic field can enhance or hinder the circular laser polarization-induced rotation. Furthermore, for the resonant case,  $\bar{\omega}=\beta$ , the electron–magnetic-field angular momentum coupling can be suppressed when equations of motion are examined in the rotating frame of the laser polarization [Eqs. (10) and (16)].

We find in general that the effect of the magnetic field is to remove the HOHG cutoff as predicted by Eq. (3) and to extend plateaus with no limit in principle due to the nonseparability of the electron Coulomb–magnetic-field Hamiltonian [16], thus resulting in continuous energy transfer to the electron in the presence of a strong laser pulse. Furthermore, for the case  $\bar{\omega}=\beta$ , where the magnetic Larmor rotation and laser-induced rotation cancel each other [Eqs. (10) and (16)], leaving only the magnetic confinement potential  $1/2\beta^2\rho^2$ , a

more efficient HOHG spectrum is usually obtained with plateaus reaching  $\sim 2U_p$  (Figs. 1 and 6). The frequency combination  $\bar{\omega} = \omega = \beta/2$  gives only *even* harmonics (Figs. 3 and 7), whereas the combination  $\bar{\omega} = \omega \neq \beta$  gives both even and odd harmonics (Figs. 4 and 8) for both laser polarization perpendicular to the internuclear axis ( $z$  axis) or in the molecular plane ( $y$ - $z$ ).

Figures 1–4 correspond to rotation of the ionized electron around the internuclear axis ( $z$  axis) in the perpendicular  $x$ - $y$  plane. Figures 5–8 correspond to rotation of the ionized electron in the plane of the molecule, i.e., the  $y$ - $z$  plane, where in principle the electron could be induced to collide with neighboring ions. This has been shown previously to create even longer HOHG plateaus, up to  $12U_p$  in energy for

molecules extended to long internuclear distances. [6,27]. The present calculations have been performed at the equilibrium distance,  $R \sim 2$  a.u., so that no marked difference has been obtained between the  $x$ - $y$  (perpendicular to internuclear axis) and  $y$ - $z$  plane (plane of the molecule) HOHG spectra. Current work in orientation dependence of HOHG in molecules suggests enhancement of the efficiency with orientation [24,28]. We have found that for circular polarization, out-of-plane (Figs. 1–4) or in-plane electron rotation (Figs. 5–8) efficiencies are comparable due to the short equilibrium distance of the molecule. Laser- and magnetic-field-induced recollision of electrons at large critical internuclear distances remains an intriguing possibility and is being examined by simulation.

- 
- [1] T. Brabec and F. Krausz, *Rev. Mod. Phys.* **72**, 545 (2000).  
 [2] P.B. Corkum, *Phys. Rev. Lett.* **71**, 1994 (1993).  
 [3] T. Zuo, S. Chelkowski, and A.D. Bandrauk, *Phys. Rev. A* **48**, 3837 (1993).  
 [4] M.Y. Ivanov, P.B. Corkum, T. Zuo, and A.D. Bandrauk, *Phys. Rev. Lett.* **74**, 2933 (1995).  
 [5] T. Zuo, A.D. Bandrauk, M.Y. Ivanov, and P.B. Corkum, *Phys. Rev. A* **51**, 3991 (1995).  
 [6] A.D. Bandrauk and H. Yu, *Phys. Rev. A* **59**, 539 (1999); *J. Phys. B* **31**, 4243 (1998).  
 [7] M. Lewenstein, P. Balcou, M.Y. Ivanov, A. L'Huillier, and P.B. Corkum, *Phys. Rev. A* **49**, 2117 (1994).  
 [8] W. Becker, S. Long, and J.K. McIver, *Phys. Rev. A* **50**, 1540 (1994).  
 [9] A.D. Bandrauk and H. Kono, in *Advances in Multiphoton Processes and Spectroscopy*, edited by S.H. Lin (World Scientific, Singapore, 2003), Vol. 15, pp. 147–214.  
 [10] M. Drescher, M. Hentschel, R. Kienberger, G. Tempea, C. Spielmann, G.A. Reider, P.B. Corkum, and F. Krausz, *Science* **291**, 1923 (2001).  
 [11] M. Hentschel *et al.*, *Nature (London)* **414**, 509 (2001).  
 [12] A.D. Bandrauk and H.S. Nguyen, *Phys. Rev. A* **66**, 031401 (2002).  
 [13] A.D. Bandrauk, S. Chelkowski, and H.S. Nguyen, *Phys. Rev. Lett.* **89**, 283903 (2002).  
 [14] T. Zuo and A.D. Bandrauk, *J. Nonlinear Opt. Phys. Mater.* **4**, 533 (1995).  
 [15] A.D. Bandrauk and H.Z. Lu, *Phys. Rev. A* **62**, 053406 (2000).  
 [16] H. Friedrich and D. Wintgen, *Phys. Rep.* **183**, 37 (1989).  
 [17] U. Kappes and P. Schmelcher, *Phys. Rev. A* **51**, 4542 (1995).  
 [18] J.R. Sabin (private communication).  
 [19] D.B. Milosevic and A.F. Starace, *Phys. Rev. A* **60**, 3160 (1999).  
 [20] G. Vignale and M. Rasolt, *Phys. Rev. Lett.* **59**, 2360 (1987).  
 [21] H.Z. Lu and A.D. Bandrauk, *J. Chem. Phys.* **115**, 1670 (2001); *J. Mol. Struct.: THEOCHEM* **547**, 97 (2001).  
 [22] A.D. Bandrauk and J. Ruel, *Phys. Rev. A* **59**, 2153 (1999).  
 [23] H. Yu and A.D. Bandrauk, *J. Chem. Phys.* **102**, 1257 (1995).  
 [24] D.G. Lappas and J.P. Marangos, *J. Phys. B* **33**, 4679 (2000).  
 [25] B.R. Johnson, J.O. Hirschfelder, and K.H. Yang, *Rev. Mod. Phys.* **55**, 109 (1983).  
 [26] K. Burnett, V.C. Reed, J. Cooper, and P.L. Knight, *Phys. Rev. A* **45**, 3347 (1992).  
 [27] A.D. Bandrauk, S. Chelkowski, H. Yu, and E. Constant, *Phys. Rev. A* **56**, R2537 (1997).  
 [28] R. Velotta, N. Hay, M.B. Mason, M. Castillejo, and J.P. Marangos, *Phys. Rev. Lett.* **87**, 183901 (2001).